

**Silver(I) complexes containing antifungal azoles: significant
improvement of the anti-*Candida* potential of the azole drug after its
coordination to the silver(I) ion**

Mia Stanković,^a Jakob Kljun,^b Nevena Lj. Stevanović,^a Jelena Lazic,^c Sanja Skaro
Bogojevic,^c Sandra Vojnovic,^c Matija Zlataar,^d Jasmina Nikodinovic-Runic,^c Iztok Turel,^{*b}
Miloš I. Djuran^{*c} and Biljana Đ. Glišić^{*a}

^a*University of Kragujevac, Faculty of Science, Department of Chemistry, R. Domanovića
12, 34000 Kragujevac, Serbia*

^b*University of Ljubljana, Faculty of Chemistry and Chemical Technology, Večna pot 113,
SI-1000 Ljubljana, Slovenia*

^c*University of Belgrade, Institute of Molecular Genetics and Genetic Engineering, Vojvode
Stepe 444a, 11042 Belgrade, Serbia*

^d*University of Belgrade-Institute of Chemistry, Technology and Metallurgy, Department of
Chemistry, Njegoševa 12, 11000 Belgrade, Serbia*

^e*Serbian Academy of Sciences and Arts, Knez Mihailova 35, 11000 Belgrade, Serbia*

*Corresponding authors.

E-mail address: Iztok.Turel@fkkt.uni-lj.si (I. Turel); milos.djuran@pmf.kg.ac.rs (M. I.
Djuran); biljana.glisic@pmf.kg.ac.rs (B. Đ. Glišić).

Abstract

Inspired by the emergence of resistance to currently available antifungal therapy and by the great potential of metal complexes for the treatment of various diseases, we synthesized three new silver(I) complexes containing clinically used antifungal azoles as ligands, $[\text{Ag}(\text{ecz})_2]\text{SbF}_6$ (**1**, ecz is econazole), $\{[\text{Ag}(\text{vcz})_2]\text{SbF}_6\}_n$ (**2**, vcz is voriconazole), and $[\text{Ag}(\text{ctz})_2]\text{SbF}_6$ (**3**, ctz is clotrimazole), and investigated their antimicrobial properties. The synthesized complexes were characterized by mass spectrometry, IR, UV-vis and ^1H NMR spectroscopy, cyclic voltammetry, and single-crystal X-ray diffraction analysis. In the mononuclear complexes **1** and **3** with ecz and ctz, respectively, the silver(I) ion has the expected linear geometry, in which the azoles are monodentately coordinated to this metal center through the N3 imidazole nitrogen atom. In contrast, the vcz-containing complex **2** has a polymeric structure in the solid state in which the silver(I) ions are coordinated by four nitrogen atoms in a distorted tetrahedral geometry. DFT calculations were done to predict the most favorable structures of the studied complexes in DMSO solution. All the studied silver(I) complexes have shown excellent antifungal and good to moderate antibacterial activities with minimal inhibitory concentration (MIC) values in the ranges of 0.01–27.1 and 2.61–47.9 μM on the selected panel of fungi and bacteria, respectively. Importantly, the complexes **1–3** have exhibited a significantly improved antifungal activity compared to the free azoles, with the most pronounced effect observed in the case of complex **2** compared to the parent vcz against *Candida glabrata* with an increase of activity by five orders of magnitude. Moreover, the silver(I)-azole complexes **2** and **3** significantly inhibited the formation of *C. albicans* hyphae and biofilms at the subinhibitory concentration of 50% MIC. To investigate the impact of the complex **3** more thoroughly on *Candida* pathogenesis, its effect on the adherence of *C. albicans* to A549 cells (human adenocarcinoma alveolar basal epithelial cells), as an initial step of the invasion of host cells, was studied.

Keywords: Silver(I) complexes; Antifungal azoles; Structural characterization; Antimicrobial activity; Biofilms

TABLE OF CONTENTS

Fig. S1 Time-dependent UV-Vis spectra of complexes 1 – 3 in DMSO at ambient temperature.	S4
Fig. S2 Time-dependent UV-Vis spectra of complexes 1 – 3 in DMSO/PBS (v/v 7 : 3) at ambient temperature.	S5
Fig. S3 ¹ H NMR spectra of econazole (ecz) and complex 1 (DMSO, 200 MHz).	S6
Fig. S4 ¹ H NMR spectra of voriconazole (vcz) and complex 2 (DMSO, 200 MHz).	S7
Fig. S5 ¹ H NMR spectra of clotrimazole (ctz) and complex 3 (DMSO, 200 MHz).	S8
Fig. S6 ESI-HRMS spectra in the positive mode of complex 1 recorded after its dissolving in CH ₃ CN. Main peaks observed can be assigned to the [Ag(ecz) ₂] ⁺ (866.9583) and eczH ⁺ (381.0385) species.	S9
Fig. S7 ESI-HRMS spectra in the positive mode of complex 2 recorded after its dissolving in CH ₃ CN. The main peak detected can be assigned to the [Ag(vcz)(MeCN)] ⁺ species (497.0447).	S10
Fig. S8 ESI-HRMS spectra in the positive mode of complex 3 recorded after its dissolving in CH ₃ CN. Main peaks observed can be assigned to the [Ag(ctz) ₂] ⁺ (795.1209) and ctzH ⁺ (277.0811) species.	S11
Fig. S9 Cyclic voltammograms of complexes 1 – 3 recorded at GC electrode in DMSO and 0.1 M TBAHP as a supporting electrolyte with a scan rate of 50 mV s ⁻¹ .	S12
Fig. S10 UV-Vis spectrophotometric ergosterol profiles between 240 and 300 nm of <i>C. albicans</i> ATCC 10231 cultures treated with 0.5 × MIC of complexes 2 and 3 , azoles vcz and ctz, and AgSbF ₆ .	S13
Fig. S11 Photographs of the analyzed crystals of complexes 1 – 3 .	S14
Fig. S12 Photograph of the crystals of 3 under the microscope (10× magnification).	S15
Table S1 The selectivity index value (SI) of silver(I) complexes 1 – 3 and the azoles on <i>Candida</i> strains	S16
Table S2 Percentage of <i>C. albicans</i> ATCC 10231 biofilm formation inhibition by treatment with 0.5 × MIC of the tested compounds after 48 h	S17
Table S3 Crystallographic data for complexes 1 – 3	S18
Spectroscopic characterization of the studied azoles	S19

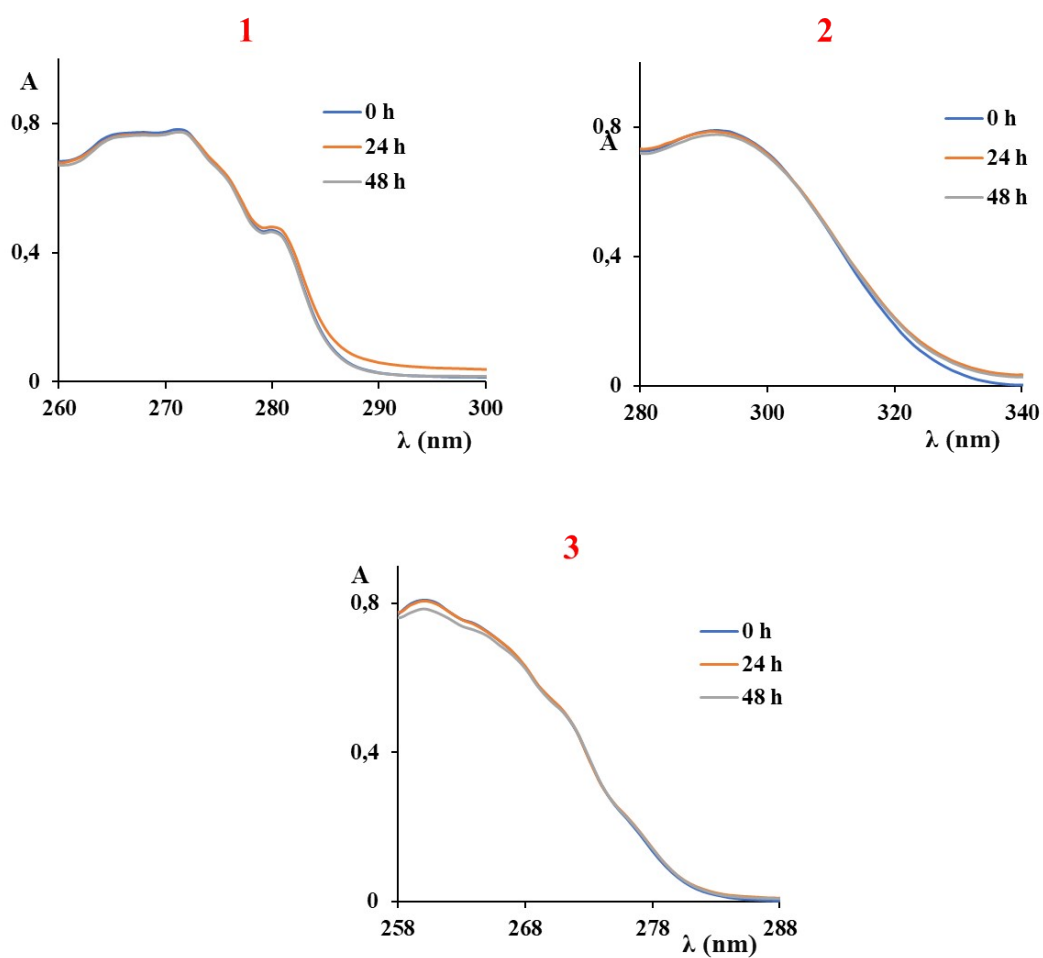


Fig. S1 Time-dependent UV-Vis spectra of complexes **1** – **3** in DMSO at ambient temperature.

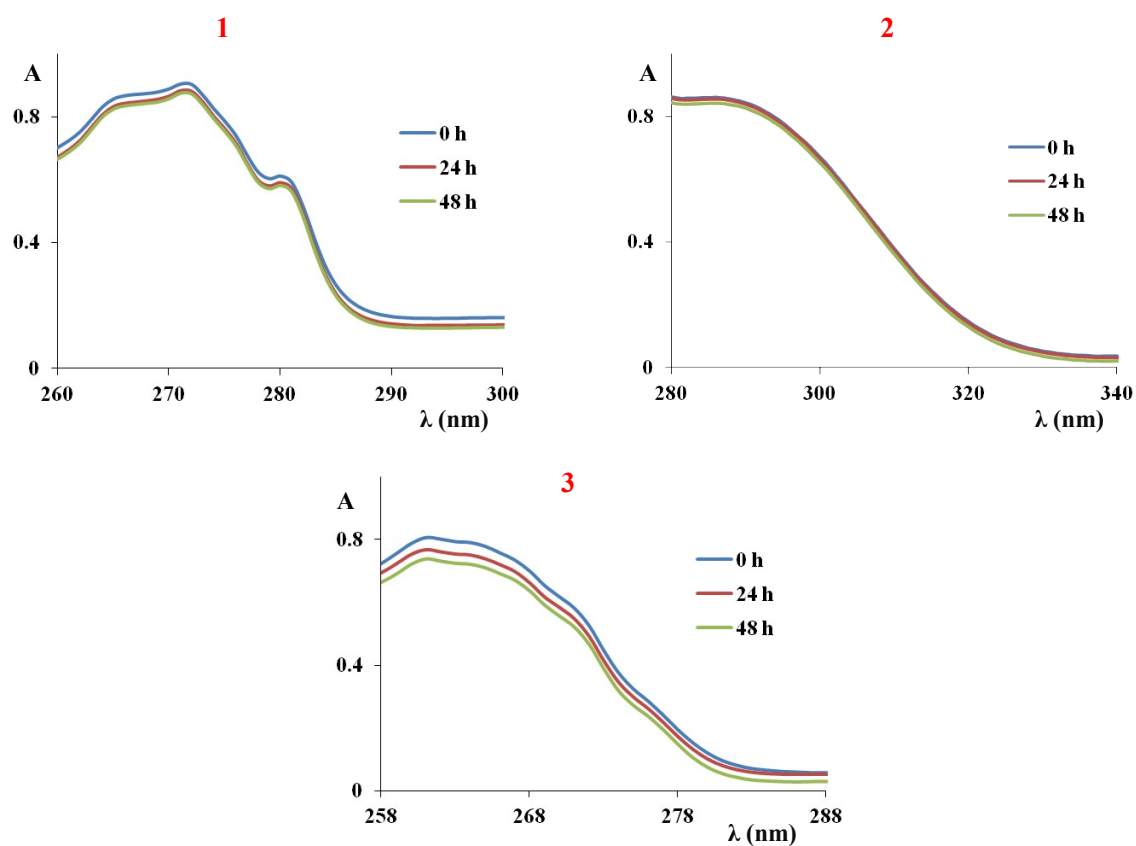


Fig. S2 Time-dependent UV-Vis spectra of complexes **1** – **3** in DMSO/PBS (v/v 7 : 3) at ambient temperature.

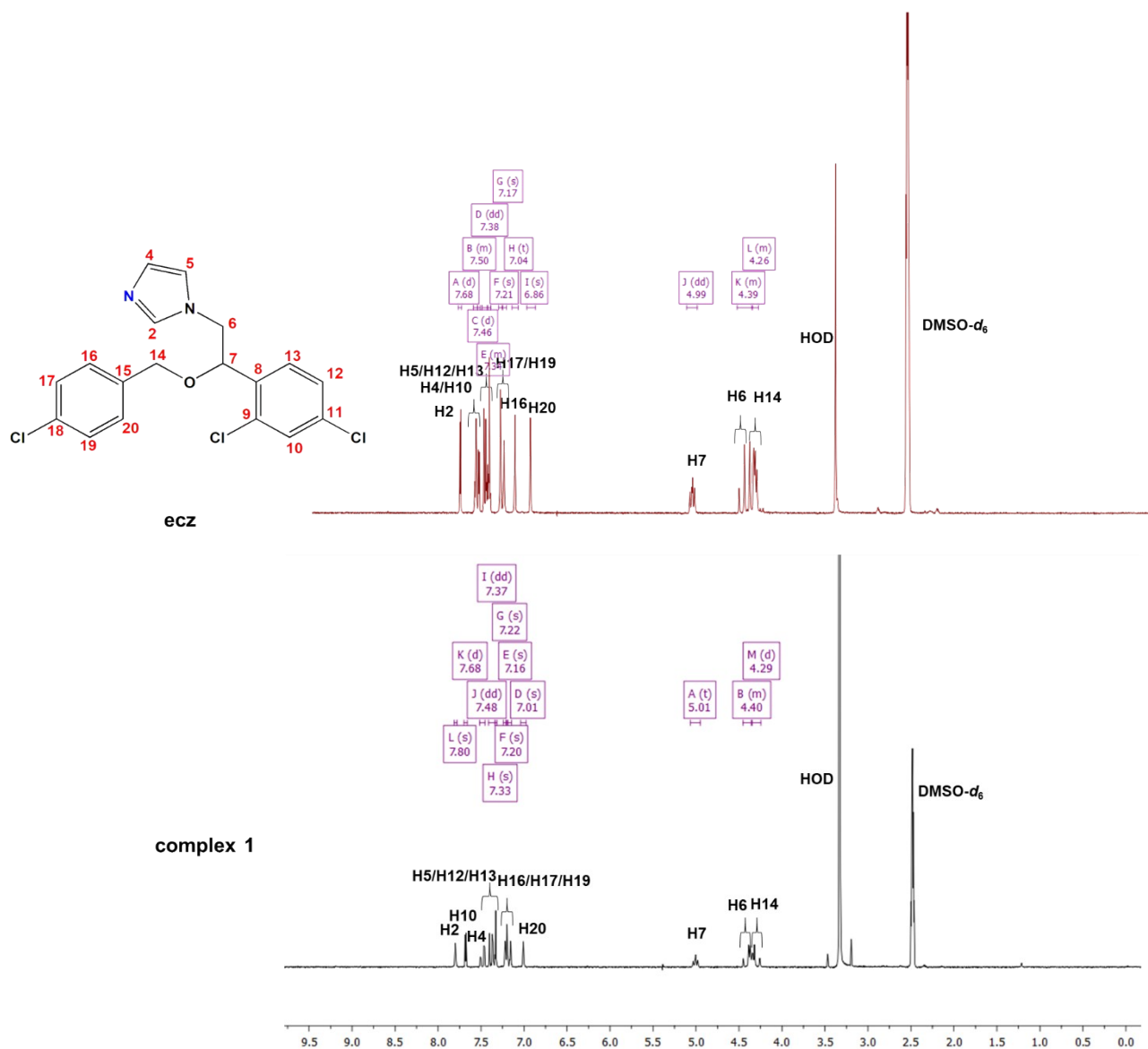


Fig. S3 ^1H NMR spectra of econazole (**ecz**) and complex **1** (DMSO, 200 MHz).

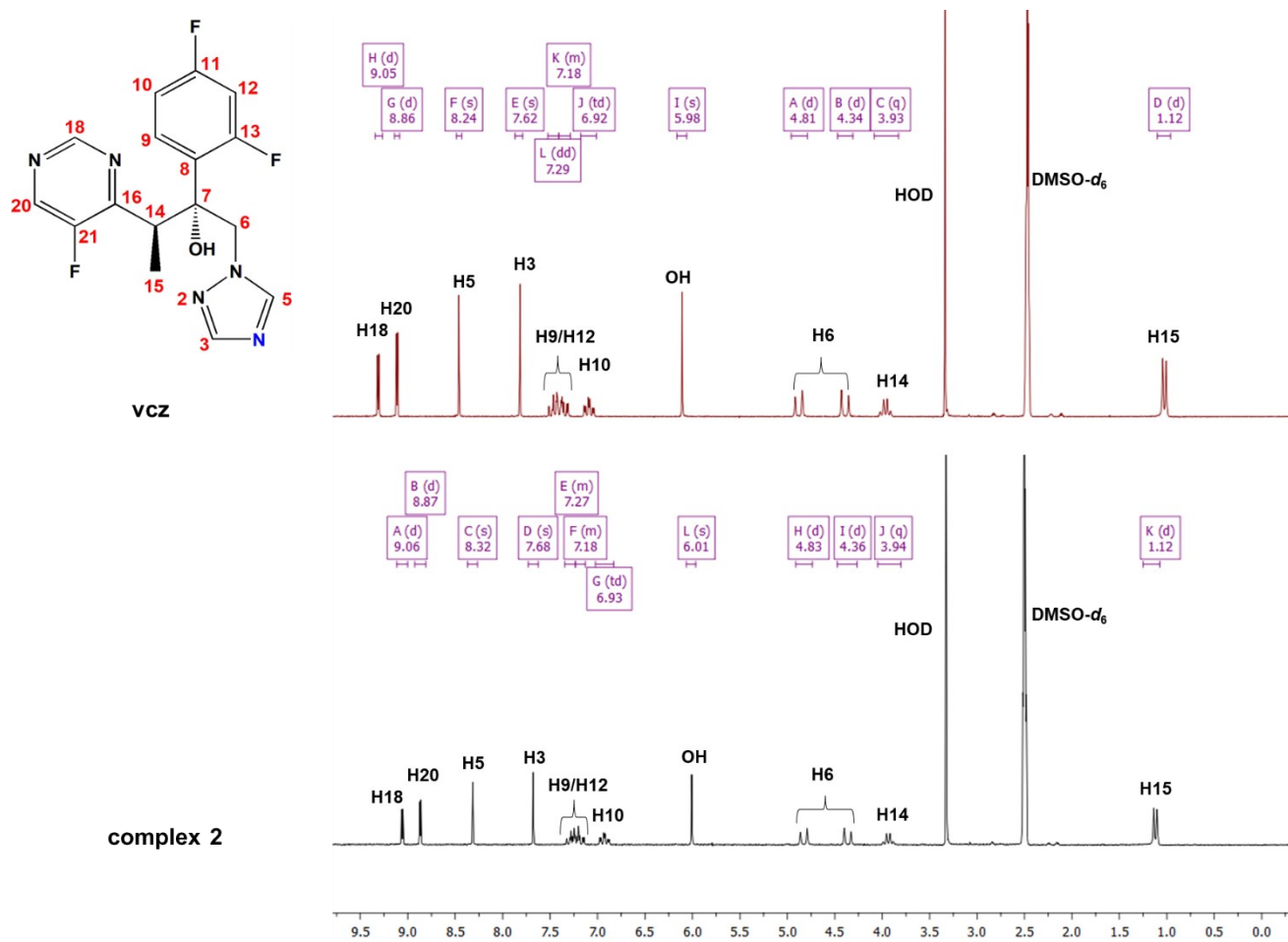


Fig. S4 ^1H NMR spectra of voriconazole (vcz) and complex 2 (DMSO, 200 MHz).

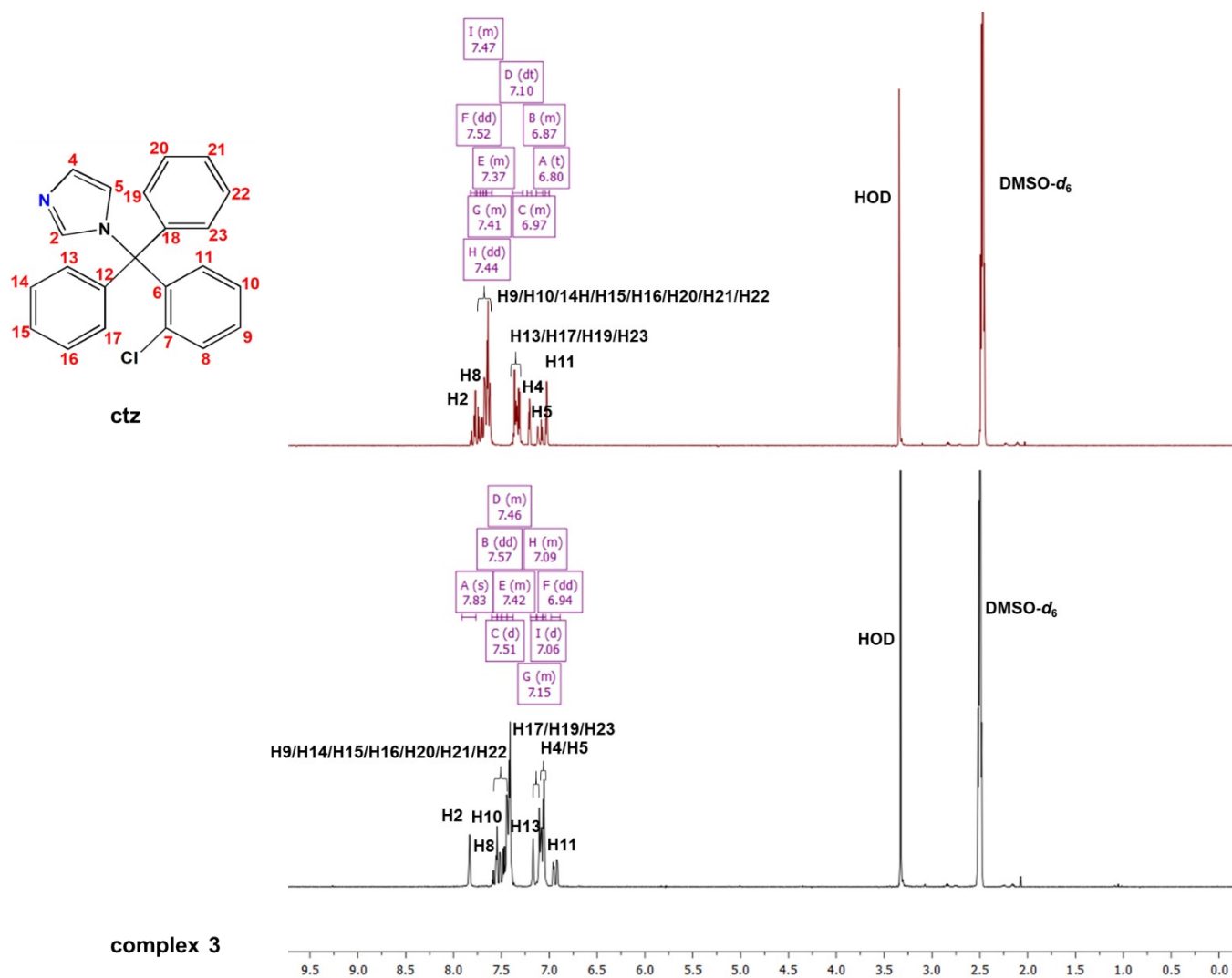
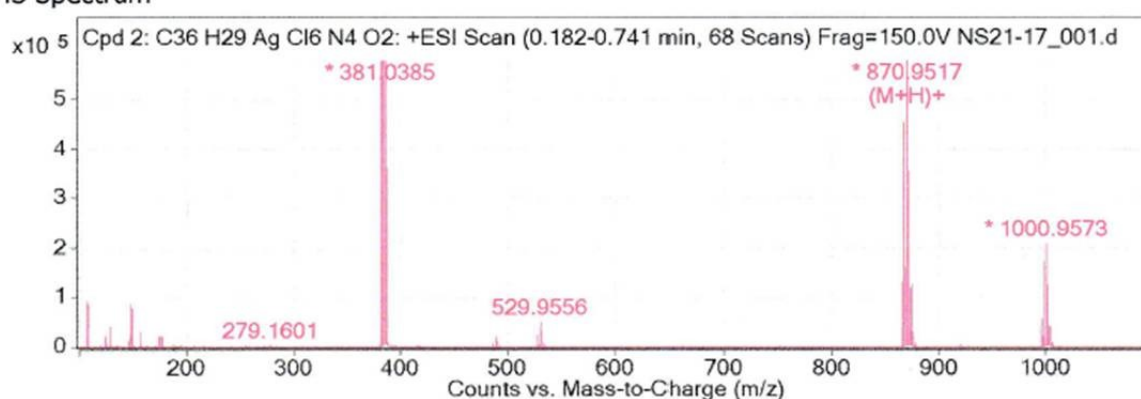


Fig. S5 ¹H NMR spectra of clotrimazole (ctz) and complex 3 (DMSO, 200 MHz).

Ion Mass	Calc Ion Mass	Difference	IonFormula	IonSpecies	Best
866.9583	866.9586	0.3	C41 H30 Ag Cl6 N2	(M+H)+	
866.9583	866.9577	-0.5	C26 H36 Ag Cl6 N3 O10	(M+H)+	
866.9583	866.9577	-0.6	C25 H30 Ag Cl6 N10 O5	(M+H)+	
866.9583	866.9591	0.8	C27 H32 Ag Cl6 N7 O6	(M+H)+	
866.9583	866.9564	-1.9	C24 H34 Ag Cl6 N6 O9	(M+H)+	
866.9583	866.9604	2.1	C29 H34 Ag Cl6 N4 O7	(M+H)+	
866.9583	866.9559	-2.4	C38 H32 Ag Cl6 N O3	(M+H)+	
866.9583	866.9617	3.5	C30 H30 Ag Cl6 N8 O3	(M+H)+	
866.9583	866.9618	3.5	C31 H36 Ag Cl6 N O8	(M+H)+	
866.9583	866.9545	-3.7	C36 H30 Ag Cl6 N4 O2	(M+H)+	✓

MS Spectrum



MFE MS Zoomed Spectrum

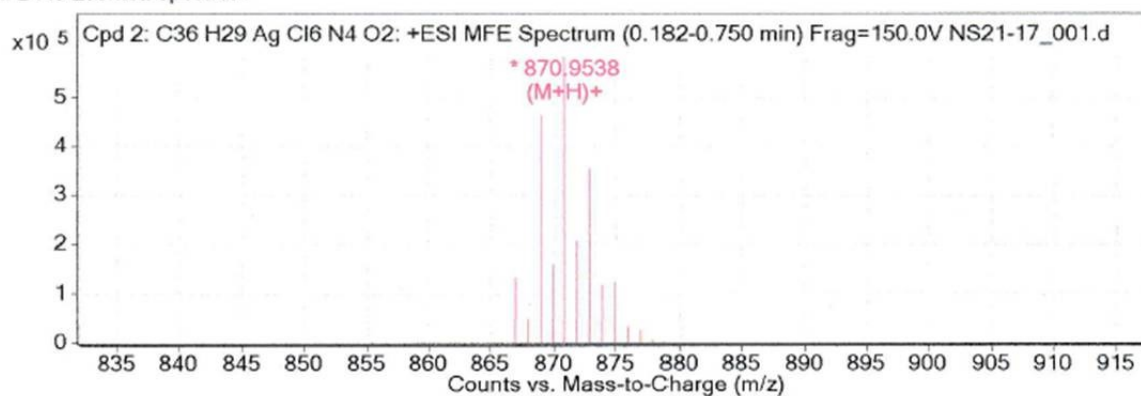
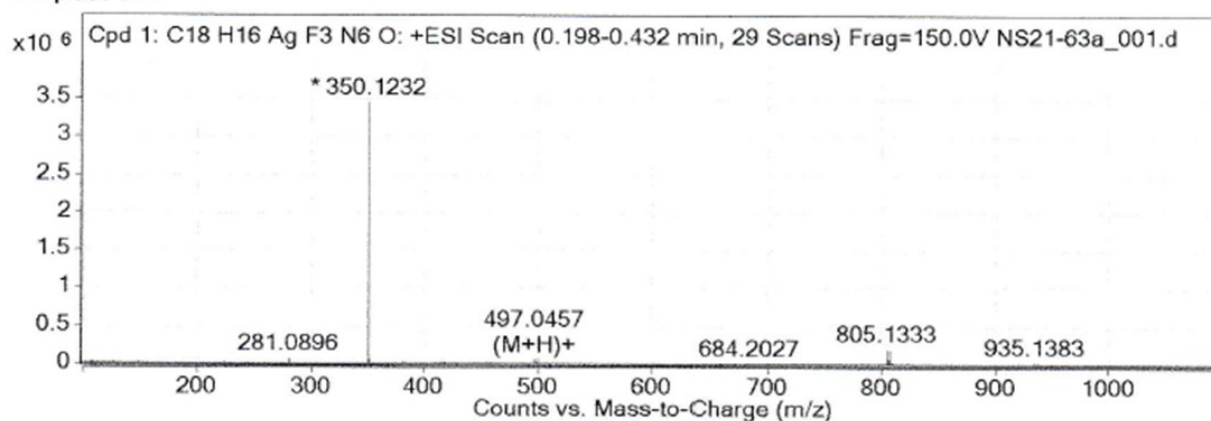


Fig. S6 ESI-HRMS spectra in the positive mode of complex **1** recorded after its dissolving in CH_3CN . Main peaks observed can be assigned to the $[\text{Ag}(\text{ecz})_2]^+$ (866.9583) and eczH^+ (381.0385) species.

Ion Mass	Calc Ion Mass	Difference	IonFormula	IonSpecies	Best
497.0447	497.0448	0.1	C17 H21 Ag F3 N2 O5	(M+H)+	
497.0447	497.0448	0.1	C16 H15 Ag F3 N9	(M+H)+	
497.0447	497.0446	-0.1	C12 H20 Ag F4 N5 O5	(M+H)+	
497.0447	497.0452	0.6	C23 H19 Ag F5	(M+H)+	
497.0447	497.0457	1.1	C9 H21 Ag F5 N5 O6	(M+H)+	
497.0447	497.0435	-1.2	C15 H19 Ag F3 N5 O4	(M+H)+	
497.0447	497.0459	1.3	C13 H16 Ag F4 N9 O	(M+H)+	
497.0447	497.0459	1.3	C14 H22 Ag F4 N2 O6	(M+H)+	
497.0447	497.0433	-1.4	C10 H18 Ag F4 N8 O4	(M+H)+	
497.0447	497.0461	1.5	C18 H17 Ag F3 N6 O	(M+H)+	✓

MS Spectrum



MFE MS Zoomed Spectrum

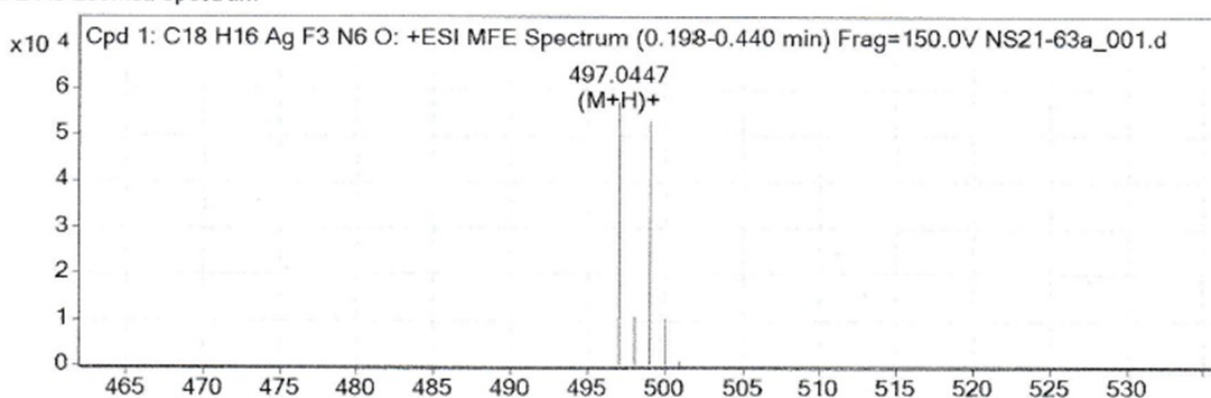
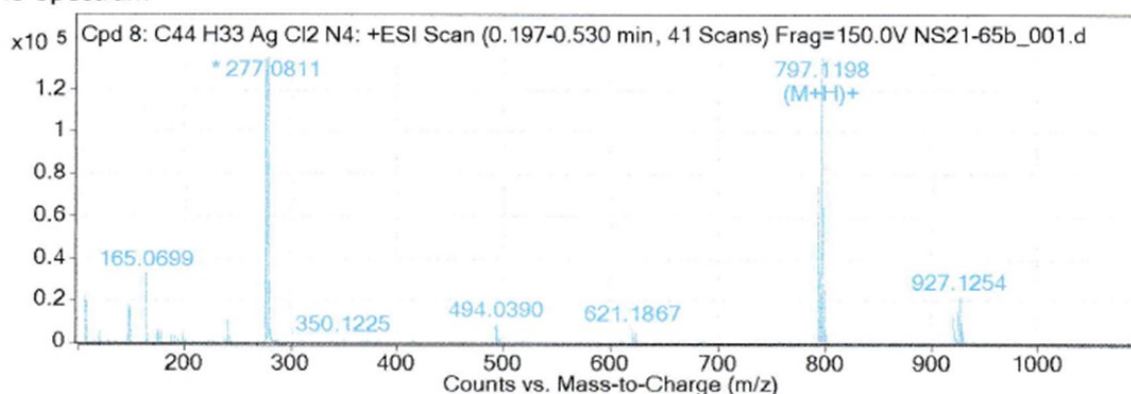


Fig. S7 ESI-HRMS spectra in the positive mode of complex **2** recorded after its dissolving in CH₃CN. The main peak detected can be assigned to the [Ag(vcz)(MeCN)]⁺ species (497.0447).

Ion Mass	Calc Ion Mass	Difference	IonFormula	IonSpecies	Best
795.1209	795.1211	0.2	C30 H36 Ag Cl2 N9 O6	(M+H)+	
795.1209	795.1206	-0.3	C44 H34 Ag Cl2 N4	(M+H)+	✓
795.1209	795.1219	1	C46 H36 Ag Cl2 N O	(M+H)+	
795.1209	795.1198	-1.1	C29 H40 Ag Cl2 N5 O10	(M+H)+	
795.1209	795.1224	1.5	C32 H38 Ag Cl2 N6 O7	(M+H)+	
795.1209	795.1193	-1.7	C43 H38 Ag Cl2 O4	(M+H)+	
795.1209	795.1238	2.9	C33 H34 Ag Cl2 N10 O3	(M+H)+	
795.1209	795.1238	2.9	C34 H40 Ag Cl2 N3 O8	(M+H)+	
795.1209	795.1179	-3	C41 H36 Ag Cl2 N3 O3	(M+H)+	
795.1209	795.1251	4.2	C35 H36 Ag Cl2 N7 O4	(M+H)+	

MS Spectrum



MFE MS Zoomed Spectrum

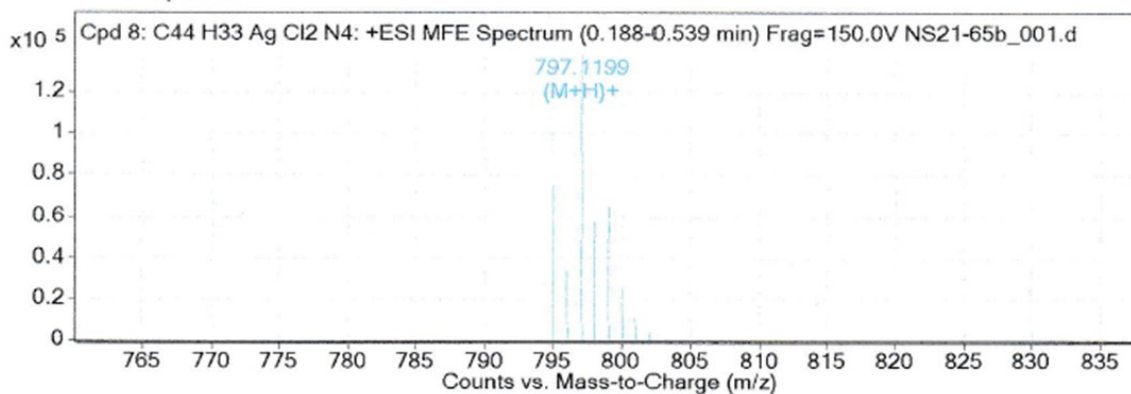


Fig. S8 ESI-HRMS spectra in the positive mode of complex **3** recorded after its dissolving in CH₃CN. Main peaks observed can be assigned to the [Ag(ctz)₂]⁺ (795.1209) and ctzH⁺ (277.0811) species.

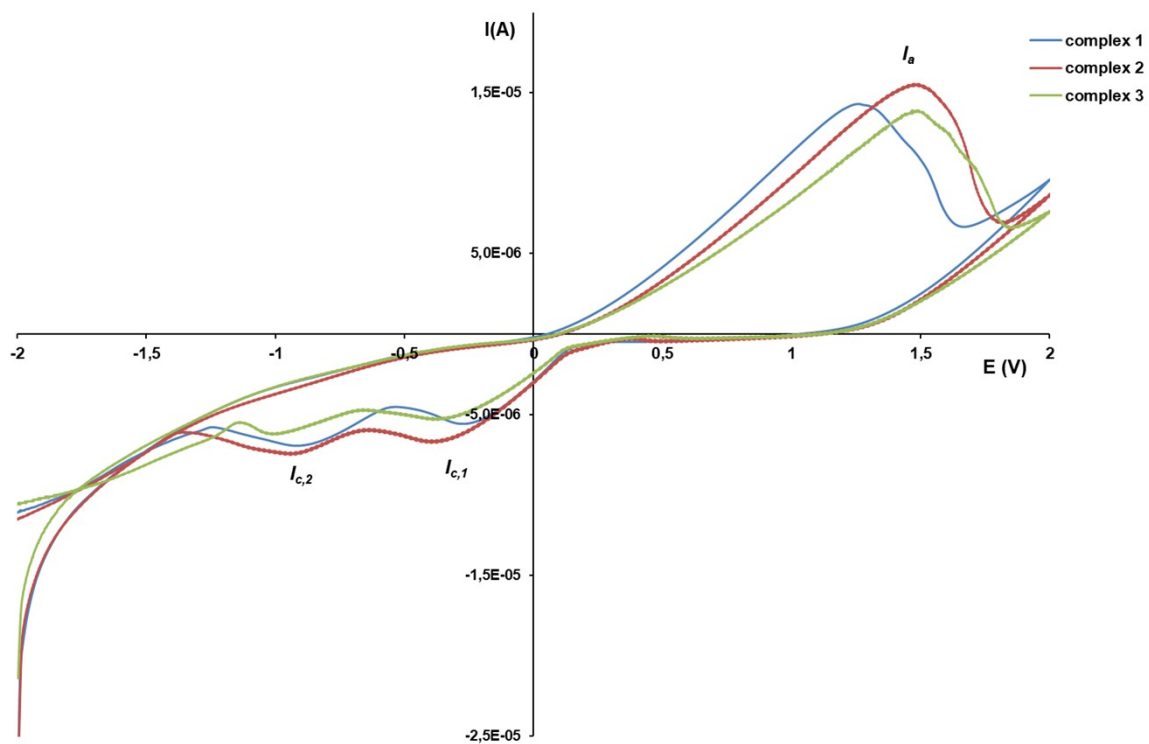


Fig. S9 Cyclic voltammograms of complexes **1** – **3** recorded at GC electrode in DMSO and 0.1 M TBAHP as a supporting electrolyte with a scan rate of 50 mV s^{-1} .

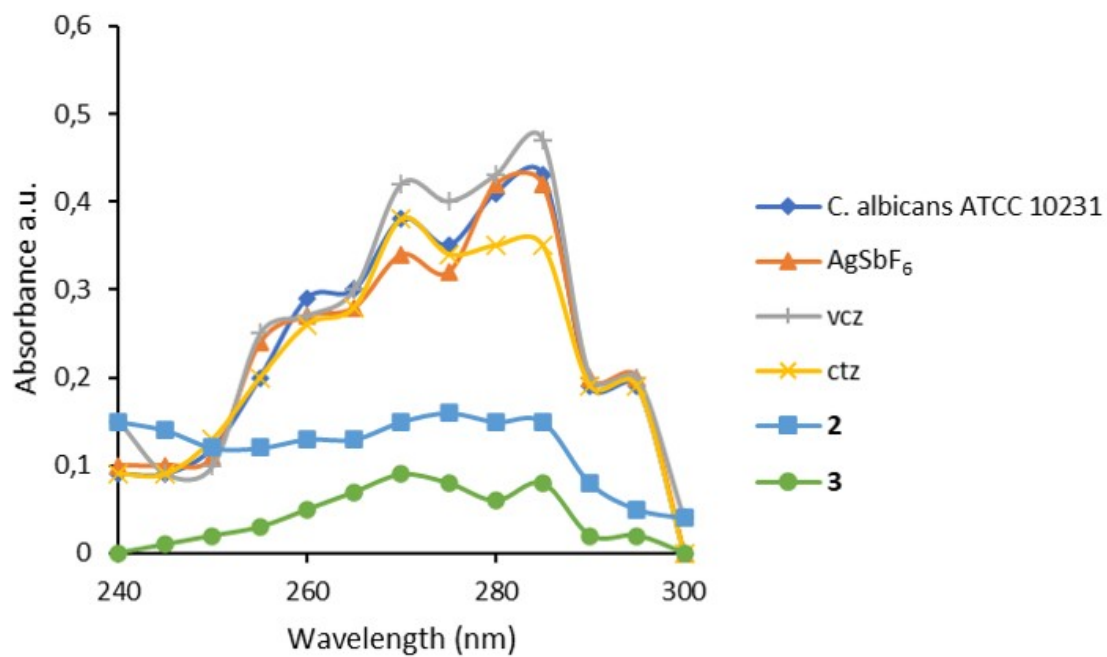


Fig. S10 UV-Vis spectrophotometric ergosterol profiles between 240 and 300 nm of *C. albicans* ATCC 10231 cultures treated with $0.5 \times$ MIC of complexes **2** and **3**, azoles vcz and ctz, and AgSbF₆.

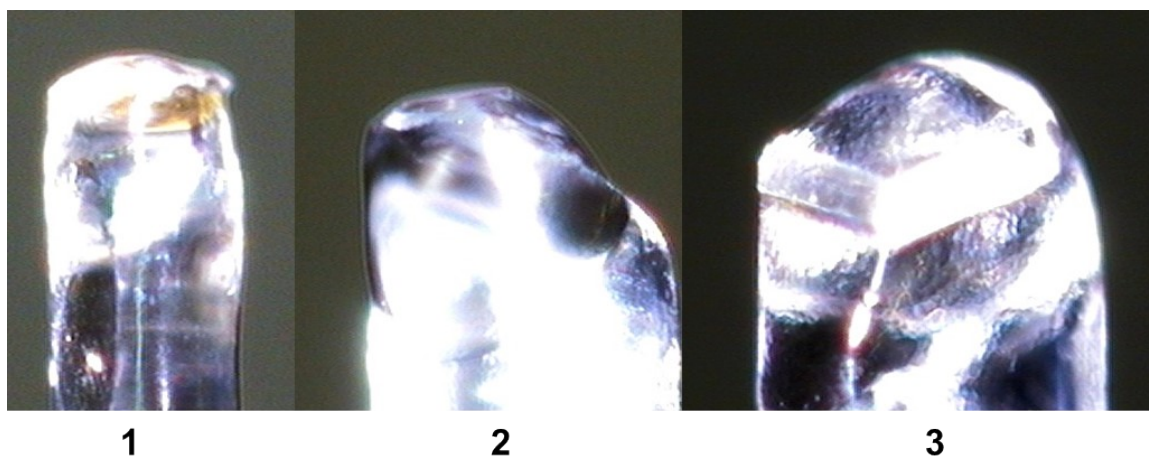


Fig. S11 Photographs of the analyzed crystals of complexes **1 – 3**.

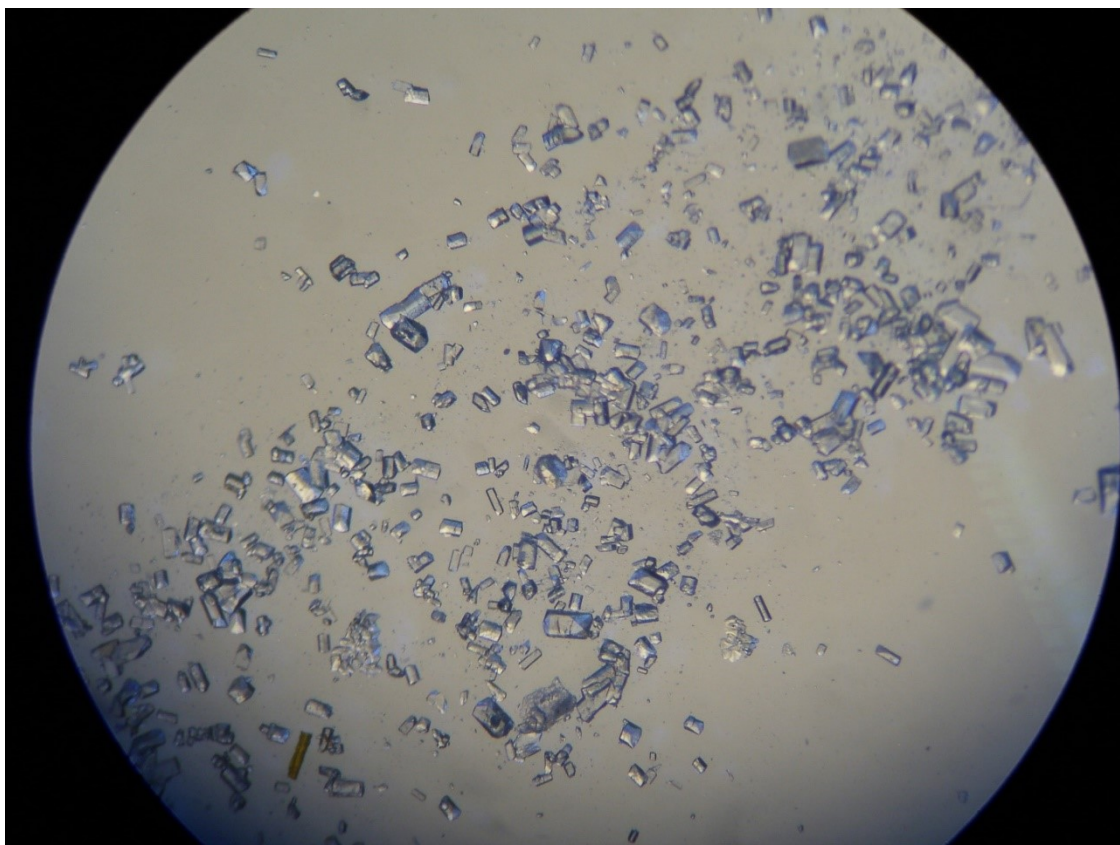


Fig. S12 Photograph of the crystals of **3** under the microscope (10× magnification).

Table S1 The selectivity index value (SI) of silver(I) complexes **1 – 3** and the azoles on *Candida* strains

Silver(I) compound/azole	Test organism	<i>C. albicans</i>	<i>C. parapsilosis</i>	<i>C. krusei</i>	<i>C. glabrata</i>
		ATCC 10231	ATCC 22019	ATCC 6258	ATCC 2001
1		4.4	4.4	<u>0.4</u>	<u>0.9</u>
econazole (ecz)		1.5	2.6	<u>0.7</u>	<u>0.2</u>
2		75.2	3610	3610	601.7
voriconazole (vcz)		24.0	2863	613.6	1.5
3		133.3	1600	533.3	16.5
clotrimazole (ctz)		3.3	<u>0.8</u>	6.2	1.0
AgSbF ₆		5.0	203.3	3.9	7.8

^athe five highest values are marked in bold, while the five lowest (not so favorable) values are underlined.

Table S2 Percentage of *C. albicans* ATCC 10231 biofilm formation inhibition by treatment with $0.5 \times$ MIC of the tested compounds after 48 h

Compounds	AgSbF ₆	2	3	vcz	ctz
% inhibition of biofilm formation	88.4 ± 3.1	87.0 ± 0.4	86.4 ± 1.3	62.5 ± 6.3	79.1 ± 3.9

Table S3 Crystallographic data for complexes 1 – 3

Complex	1	2	3
CCDC No.	2277941	2277943	2277942
Empirical formula	C ₃₆ H ₃₀ AgCl ₆ F ₆ N ₄ O ₂ Sb	C ₃₂ H ₂₈ AgF ₁₂ N ₁₀ O ₂ Sb	C ₄₄ H ₃₄ AgCl ₂ F ₆ N ₄ Sb
Formula weight [g mol ⁻¹]	1106.96	1042.26	1033.27
Temperature [K]	150.00(10)	150.00(10)	150.00(10)
Crystal system	monoclinic	triclinic	orthorhombic
Space group	P2 ₁ /n	P1	Fdd2
a [Å]	15.8651(10)	6.4313(3)	31.1679(12)
b [Å]	9.0452(4)	9.8300(5)	30.6135(11)
c [Å]	16.4734(12)	15.7404(5)	8.4227(5)
α [°]	90	100.272(3)	90
β [°]	118.245(9)	99.905(3)	90
γ [°]	90	97.173(4)	90
Volume [Å ³]	2082.5(3)	952.05(7)	8036.7(6)
Z	2	1	16
ρ _{calc} [g cm ⁻³]	1.765	1.818	1.708
μ [mm ⁻¹]	1.569	1.328	1.359
F(000)	1088.0	512.0	4096.0
Crystal size [mm ³]	0.2 × 0.05 × 0.05	0.1 × 0.1 × 0.025	0.15 × 0.1 × 0.01
Radiation	Mo Kα (λ = 0.71073)	Mo Kα (λ = 0.71073)	Mo Kα (λ = 0.71073)
2θ range for data collection [°]	4.91 to 54.966	5.368 to 54.964	5.184 to 54.95
Index ranges	-20 ≤ h ≤ 20, -11 ≤ k ≤ 11, -20 ≤ l ≤ 21	-8 ≤ h ≤ 8, -12 ≤ k ≤ 12, -20 ≤ l ≤ 20	-38 ≤ h ≤ 40, -24 ≤ k ≤ 38, -8 ≤ l ≤ 10
Reflections collected	17804	14307	9529
Independent reflections	4711 [R _{int} = 0.0365, R _{sigma} = 0.0384]	7998 [R _{int} = 0.0355, R _{sigma} = 0.0577]	3778 [R _{int} = 0.0170, R _{sigma} = 0.0175]
Data/restraints/parameters	4711/0/256	7998/57/527	3778/3/273
Goodness-of-fit on F ²	1.031	0.994	1.093
Final R indexes [I ≥ 2σ (I)]	R ₁ = 0.0434, wR ₂ = 0.0994	R ₁ = 0.0306, wR ₂ = 0.0540	R ₁ = 0.0252, wR ₂ = 0.0566
Final R indexes [all data]	R ₁ = 0.0757, wR ₂ = 0.1125	R ₁ = 0.0361, wR ₂ = 0.0562	R ₁ = 0.0286, wR ₂ = 0.0582
Largest diff. peak / hole [e Å ⁻³]	0.97/-0.78	0.35/-0.55	0.30/-0.61

Spectroscopic characterization of the studied azoles

Econazole (ecz). MW = 381.68 g mol⁻¹. IR (KBr, ν , cm⁻¹): 3115w, 3091w, 3064w ($\nu(\text{C}_{\text{diazole}}\text{-H})$ and $\nu(\text{C}_{\text{ar}}\text{-H})$), 2981w, 2969w, 2946w ($\nu(\text{C-H})$), 1590m, 1564m, 1505s, 1489s, 1473m, 1432m ($\nu(\text{C}_{\text{ar}}=\text{C}_{\text{ar}})$ and $\nu(\text{C=N})$), 1233s, 1200m ($\beta(\text{C}_{\text{ar}}\text{-H})$ and $\beta(\text{C}_{\text{diazole}}\text{-H})$), 1107s ($\nu(\text{C-O})$), 1090vs, 1046m, 1032m ($\nu(\text{C}_{\text{ar}}\text{-Cl})$), 800m, 787m, 733m, 661m, 626m ($\gamma(\text{C}_{\text{ar}}\text{-H})$) and ($\gamma(\text{C}_{\text{diazole}}\text{-H})$). ¹H NMR (200 MHz, DMSO-*d*₆): δ = 7.68 (*d*, *J* = 2.0 Hz, 1H, C2H), 7.50 (*m*, 1H, C4H), 4.56 (*d*, *J* = 2.0 Hz, 1H, C10H), 7.38 (*dd*, *J* = 4.8, 2.8 Hz, 2H, C5H, C13H), 7.34 (*m*, 1H, C12H), 7.21 (*s*, 1H, C17H), 7.17 (*s*, 1H, H19), 7.04 (*t*, *J* = 1.1 Hz, 1H, C16H), 6.86 (*s*, 1H, C20H), 4.99 (*dd*, *J* = 6.4, 4.4 Hz, C7H), 4.39 (*m*, 2H, C6H), 4.26 ppm (*m*, 2H, C14H). UV-Vis (DMSO, λ_{max} , nm): 255 (ϵ = 4.1 × 10³ M⁻¹cm⁻¹).

Voriconazole (vcz). MW = 349.31 g mol⁻¹. IR (KBr, ν , cm⁻¹): 3196br ($\nu(\text{O-H})$), 3120w, 3047w, 3017w ($\nu(\text{C}_{\text{triazole}}\text{-H})$ and $\nu(\text{C}_{\text{ar}}\text{-H})$), 2995w, 2979w, 2941w ($\nu(\text{C-H})$), 1619s, 1587vs, 1507s, 1496vs, 1451vs, 1408vs ($\nu(\text{C}_{\text{ar}}=\text{C}_{\text{ar}})$ and $\nu(\text{C=N})$), 1278s ($\delta(\text{O-H})$), 1249m, 1210m ($\beta(\text{C}_{\text{ar}}\text{-H})$ and $\beta(\text{C}_{\text{triazole}}\text{-H})$), 1132s ($\nu(\text{C-F})$), 1054m ($\nu(\text{C-O})$), 858s, 825w, 787w, 779m, 724m, 718m ($\gamma(\text{C}_{\text{ar}}\text{-H})$) and ($\gamma(\text{C}_{\text{triazole}}\text{-H})$), 622m ($\beta(\text{C}_{\text{ar}}\text{-F})$). ¹H NMR (200 MHz, DMSO-*d*₆): δ = 9.05 (*d*, *J* = 2.9 Hz, 1H, C18H), 8.86 (*d*, *J* = 2.2 Hz, 1H, C20H), 8.24 (*s*, 1H, C5H), 7.62 (*s*, 1H, C3H), 7.29 (*dd*, *J* = 9.0, 6.9 Hz, 1H, C9H), 7.18 (*m*, 1H, C12H), 6.92 (*td*, *J* = 8.6, 2.4 Hz, 1H, C10H), 5.98 (*s*, 1H, OH), 4.81 (*d*, *J* = 14.3 Hz, 1H, C6H), 4.34 (*d*, *J* = 14.3 Hz, C6H), 3.93 (*q*, *J* = 6.9 Hz, C14H), 1.12 (*d*, *J* = 7.0 Hz 3H, C15H). UV-Vis (DMSO, λ_{max} , nm): 256 (ϵ = 8.6 × 10³ M⁻¹cm⁻¹).

Clotrimazole (ctz). MW = 344.84 g mol⁻¹. IR (KBr, ν , cm⁻¹): ~3000w ($\nu(\text{C}_{\text{triazole}}\text{-H})$ and $\nu(\text{C}_{\text{ar}}\text{-H})$), 2970w ($\nu(\text{C-H})$), 1673m, 1566m, 1547m, 1494m, 1467m, 1443m ($\nu(\text{C}_{\text{ar}}=\text{C}_{\text{ar}})$ and $\nu(\text{C}_{\text{ar}}=\text{N})$), w ($\delta(\text{CH}_2)$), 1262m ($\nu(\text{C-N})$), 1210m ($\beta(\text{C}_{\text{ar}}\text{-H})$ and $\beta(\text{C}_{\text{triazole}}\text{-H})$), 1114vs, 1081s, 1041m ($\beta(\text{C}_{\text{ar}}\text{-H})$), 903m ($\beta(\text{C}_{\text{triazole}}\text{-H})$), 824m ($\delta(\text{C-N})$), 765s ($\gamma(\text{C}_{\text{ar}}\text{-H})$), 672s ($\gamma(\text{C}_{\text{ar}}\text{-H})$), 660m

Electronic Supplementary Information

(triazole ring def.), 633s (v(C–Cl)), 529m (ring def.). ¹H NMR (200 MHz, DMSO-*d*₆): δ = 7.52 (*dd*, *J* = 4.2, 3.1 Hz, 1H, C2H), 7.47 (*m*, 1H, C8H), 7.44 (*dd*, *J* = 2.5, 1.3 Hz, 1H, C10H), 7.41 (*m*, 2H, C14H, C15H) 7.37 (*m*, 5H, C9H, C16H, C20H, C21H, C22H), 7.10 (*dt*, *J* = 5.3, 2.1 Hz, 4H, C13H, C17H, C19H, C23H), 6.97 (*m*, 1H, C4H), 6.87 (*m*, 1H, C5H), 6.80 ppm (*t*, *J* = 1.4 Hz, 1H, C11H). UV-Vis (DMSO, λ_{max}, nm): 255 (ε = 7.9 × 10³ M⁻¹cm⁻¹).